An X-ray Photoelectron Spectroscopic Study of Multilayers of an Electroactive Ferrocene Derivative Attached to Platinum and Gold Electrodes

Alan B. Fischer,[1a] Mark S. Wrighton,*[1a] M. Umanā,[1b] and Royce W. Murray*[1b]

Contribution from the Department of Chemistry, Massachusetts Institute of Technology, Cambridge, Massachusetts 02139, and the Kenan Laboratories of Chemistry, University of North Carolina, Chapel Hill, North Carolina 27514. *Received October 3, 1978*

Abstract: Pretreated (anodized) Pt and Au electrode surfaces derivatized with (1,1′-ferrocenediyl)dichlorosilane have been analyzed by X-ray photoelectron spectroscopy (XPES). The derivatized surfaces exhibit Fe $2p_{3/2}$ bands with binding energies consistent with ferrocene iron and with large companion satellite peaks. Using a layer model, relative Fe $2p_{3/2}$ and electrode substrate intensities (Au or Pt) can be correlated with ferrocene coverage measured by cyclic voltammetry. The results indicate that electrochemical charge transfer can occur through ferrocene/silane layers of thicknesses exceeding 100 Å. XPES data indicate that the attached electroactive material contains less than the expected 1:1 ratio of Fe:Si, indicating some ferrocene degradation in the attachment procedure. These surface analyses accord well with elemental analyses of hydrolyzed material resulting from reaction of H_2O with (1,1′-ferrocenediyl)dichlorosilane which also shows less than a 1:1 Fe:Si ratio.

Our laboratories have recently described the attachment of organosilane reagents to the surfaces of oxidized platinum electrodes[2a] and the electrochemistry of surfaces which result from reaction of (1,1′-ferrocenediyl)dichlorosilane (I) with

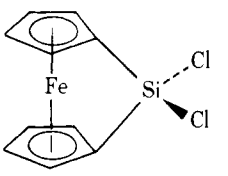

I

oxidized Pt and Au electrodes.[2b,3] Appropriately pretreated Au and Pt electrodes derivatized with I exhibit cyclic voltammetric waves at a potential which is within 100 mV of the formal potential for the ferricenium/ferrocene couple. These waves have properties expected[4] of an electroactive moiety persistently attached to the electrode surface in both oxidized and reduced forms. The waves are quite persistent to repeated cyclical oxidation–reduction, and the charge under the waves corresponds to quite large and variable (from electrode to electrode) coverage (Γ = 4–280 × 10^{-10} mol/cm^2) of the electrode surface by electroactive ferrocene. Coverages of these magnitudes require an interpretation involving a multilayer arrangement of ferrocene; e.g., it is probable that oligomerization of I occurs coincident with the electrode attachment reaction. The ability of such multilayered structures to undergo chemically reversible and, on certain electrodes, nearly electrochemically reversible ($\Delta E_{peak} \leq 10$ mV) reactions makes further study of these electrode materials of interest. In particular, the surface structural heterogeneity, implied by the variability in broadness and ΔE_{peak} of the cyclic voltammetric peaks, is a property of interest which can be studied by various surface-sensitive physical methods. The present report describes the application of X-ray photoelectron spectroscopy (XPES) to a series of oxidized Pt and Au electrodes which have been reacted with I. The data serve to confirm the presence of the ferrocene moiety and establish a rough, but positive, correlation between the quantity of ferrocene iron as detected electrochemically and by XPES.

Experimental Section

Preparation of Electrodes and Electrochemistry. The ferrocene derivative I was that used in previous studies.[2b,3] Three sets of derivatized surfaces (two Pt and one Au) have been studied. Gold or platinum foil (0.01 mm thick) was used to prepare an electrode such that both sides of ~6 × 40 mm of surface were exposed. After the electrode was cleaned in concentrated HNO_3 a 6 × 6 mm section (appropriate to mounting on the 0.25-in. XPES probe) was cut from the electrode as representative of a "clean" surface. The electrode was then pretreated according to previously[2b,3] established procedures and a second section (6 × 6 mm) of the foil strip, representative of the "pretreated surface", was removed from the electrode. The remaining portion of the foil electrode was derivatized with I as described previously. The electrode was then characterized by cyclic voltammetry in 0.1 M [n-Bu_4N]ClO_4/CH_3CN. A PAR 173/175 instrument with a Houston X-Y recorder was used. The reference electrode was an aqueous SCE. Three 6 × 6 mm sections were cut off the foil with a cyclic voltammogram before and after scission. In this manner the amount of electroactive material on each severed section can be determined. The three severed sections were washed thoroughly with CH_3CN and dried. The electrode itself was stored in air at 298 K until after XPES analyses were performed as a control to ensure prolonged attachment of the electroactive material. All samples for XPES analyses were shipped to Chapel Hill from Cambridge; two of the three derivatized sections were analyzed and one was returned to Cambridge for analysis by cyclic voltammetry to ensure surface integrity during the transit. All control samples of derivatized surfaces exhibited essentially the same cyclic voltammetric behavior (peak positions, width, and integrated area) before and after the round trip to Chapel Hill. In some cases the time period involved exceeded 8 weeks.

Hydrolysis of I. XPES of the solid obtained from reaction of I with H_2O represents a useful comparison for XPES of surfaces derivatized with I. Hydrolysis was effected either by exposing a 2-mL isooctane solution of ~50 mg of I to atmospheric moisture and shaking for 24 h at 298 K or by injecting 0.5 mL of liquid H_2O into a 2-mL isooctane solution of ~50 mg of I and shaking for 3 h at 298 K. The solid material was collected by filtration and washed with isooctane and H_2O. The solid was then dried under vacuum. Three such sets of samples were prepared; one set was analyzed by XPES and two sets were analyzed by elemental analysis by Galbraith giving Fe/Si = 0.34 (av); C/Fe = 26 (av).

X-ray Photoelectron Spectroscopy. XPES spectra were obtained on a Du Pont Model 650B electron spectrometer[5] equipped with a microprocessor system[6] which controls preprogrammed spectral acquisition and tape storage. A TV screen operator-controlled cursor allows for base line specification and automatic calculation of band (area) intensities. While smoothing capabilities exist, spectra presented here have not been smoothed. To minimize charging effects, electrodes were mounted on the spectrometer probe using conducting Ag paint. Standard compounds were run as powders on sticky tape with binding energies referenced to C 1s as 285.0 eV.

Results and Discussion

Electrochemical properties of the Pt and Au electrodes derivatized with I were similar to those discussed earlier.[2,3] Formal potentials, peak potential separations, and electroactive coverages are given in Table I. Both coverage and general

0002-7863/79/1501-3442$01.00/0

Table I. Electroanalytical and XPES Characterization of Derivatized Pt and Au Surfaces

expt no.	elec-trode	electroanalytical data[a] $E^{\circ\prime}$, V vs. SCE	ΔE_{peak}, mV	Γ, mol/cm^2 × 10^9	XPES binding energy, eV[b] Fe $2p_{3/2}$[c]	Si 2s[d]	O 1s	M $4f_{7/2}$[e]	XPES intensities I_{Fe}/I_M	I_{Fe}/I_{Si}	I_O/I_M	I_C/I_M	I_{M/M^e}[f]	layer thickness, Å d (eq 1)[f]	d (eq 2)[f]	d (eq 3)[f]
1-Pt	A	0.455	50	4.1	707.8	153.2	532.4	70.4	0.176		2.15	2.67	0.103	84	60	71
1-Pt	B	0.450	40	2.7	708.2	153.9	532.7	70.9	0.136		2.02	2.76	0.093	88	51	47
2-Pt	C	0.445	70	1.7	707.8	153.6	532.4	71.2	0.083	2.18	0.70	0.51	0.554	22	36	30
2-Pt	D	0.450	60	2.3		153.4	532.3	71.2	0.101	2.44	0.78	0.73	0.410	33	41	40
3-Au	E	0.455	60	9.5	707.9	153.5	532.4	84.0	1.597	2.35	10.75	9.10	0.036_5	122	141	166
3-Au	F	0.455	40	5.8	707.8	153.9	542.4	84.2	0.774	2.49	4.75	3.92	0.0789	94	114	101
		av 0.452	53		707.9	153.6	532.4			2.37						

[a] All electroanalytical data are from cyclic voltammetry at 0.1 V/s in 0.1 M $[(n\text{-Bu})_4N]ClO_4$ in CH_3CN solvent, $E^{\circ\prime}$ is the average of anodic and cathodic peak potential. ΔE_{peak} is the separation of anodic and cathodic peak; ΔE_{peak} diminishes at lower scan rates. Γ is coverage of electroactive material from integration of anodic peak. [b] Corrected to C 1s = 285.0 eV. [c] Value given is for the main, sharp Fe $2p_{3/2}$ peak. See Figure 3 and text for energy loss satellite. [d] The normally more useful Si 2p band is obscured by the Pt, Au base line. [e] M is Pt for electrodes A-D, Au for electrodes E and F: $\sigma(Pt\ 4f_{5/2+7/2}) = 15.84$; $\sigma(Au\ 4f_{5/2+7/2}) = 17.47$. [f] See text.

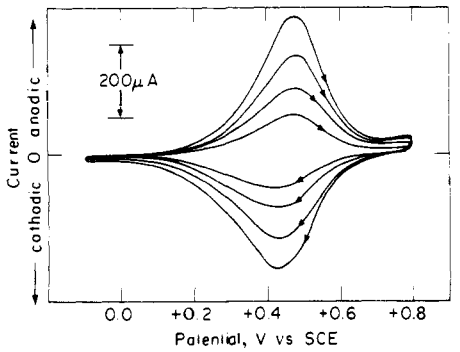

Figure 1. Cyclic voltammograms for Pt strip derivatized with I at 100 mV/s in CH_3CN, 0.1 M $[n\text{-Bu}_4N]ClO_4$. A portion of the electrode was severed after each scan and these three severed portions were shipped to Chapel Hill for surface analysis. The differences in the integrated areas of the cyclic voltammograms were used to determine the coverage of electroactive material on the severed portions.

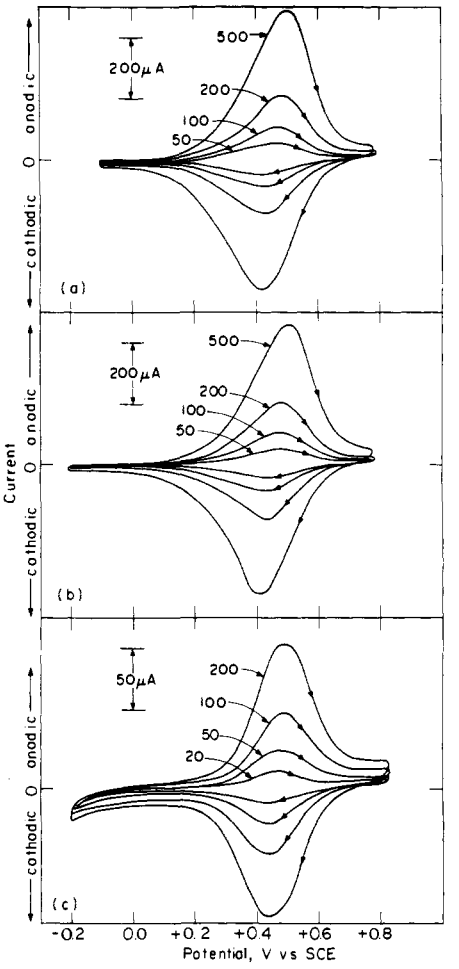

Figure 2. Cyclic voltammograms of CH_3CN, 0.1 M $[n\text{-Bu}_4N]ClO_4$, as a function of scan rate for the remaining portion of the electrode in Figure 1: (a) before sending severed portions to Chapel Hill; (b) after receiving surface analysis results (6 weeks of storage in air). The cyclic voltammograms in (c) are for one of the severed portions sent to Chapel Hill and returned to Cambridge ~6 weeks later as a control for the two portions subjected to surface analysis. Scan rate indicated are mV/s.

appearance of the cyclic voltammograms, Figures 1 and 2, indicate that the trans-shipment arrangements were satisfactory to protect the chemically modified surfaces.

All electrodes were examined at high resolution in XPES for Fe $2p_{3/2}$, N 1s, O 1s, Si 2s, Pt and Au $4f_{5/2,7/2}$, C 1s, and Cl 2p. Survey scans detected no extraneous peaks. The complete absence of Cl 2p demonstrates that the reactive Si-Cl functionalities of I react completely as expected from their hydrolytic instability. The N 1s background present on all derivatized electrodes was consistently two to four times lower than on unreacted electrodes, consistent with preempting of electrode adsorption sites for nitrogeneous contaminants. Binding energy and intensity data are given in Table I. Table II contains binding energy and intensity data for some substituted ferrocenes for comparison. Examination of Fe $2p_{3/2}$ binding energies in ferrocene standards reveals a modest sensitivity to substituent. The electrodes to which I had been attached all exhibited prominent Fe $2p_{3/2}$ spectra as illustrated in Figure 3, curves 1-3. On five of the six electrodes examined, a Fe $2p_{3/2}$ peak was clearly visible at 707.9 ± 0.1 eV. On two of the electrodes (A and B) this peak had the same shape as ferrocenes such as 1,1′-ferrocenedicarboxylic acid (Figure 3, curves 3 and 4). The 707.9-eV binding energy corresponds quite well to that observed for ferrocene in polymerized samples of I, Table II, which in turn lies within a range of energies compatible with ferrocene iron. This result confirms the expectation of the electrochemical behavior, that a ferrocene iron moiety has been attached to the surface of the Pt and Au electrodes.

A diffuse Fe $2p_{3/2}$ satellite band at 3-3.3 eV higher apparent binding energy than the main peak appears, erratically (Figure 3, curves 1-3), in the spectra of the surface-attached ferrocenes. Electrode D showed mostly this satellite; the 707.9-eV band was barely visible. The satellite amplitude exhibits no particular pattern with coverage, etc. The cyclic voltammetric behavior of these multilayer ferrocene electrodes suggests,[2b] however, that the chemical environment of the attached ferrocene can vary both within the polymer structure for a given electrode and from electrode to electrode. The satellite was also

Table II. XPES of Ferrocene Standards

sample	binding energy, eV[a]			XPES intensities[b]	
	Fe $2p_{3/2}$	Si 2s	Si 2p	I_{Fe}/I_{Si}	I_{Si2s}/I_{Si2p}
$[Fe(\eta^5\text{-}C_5H_4SiMe_3)_2]BF_4$[c]	710.6	152.1		4.53	
$Fe(\eta^5\text{-}C_5H_5)(\eta^5\text{-}C_5H_4COMe)$	708.8				
$Fe(\eta^5\text{-}C_5H_4COOH)_2$	708.6				
$Fe(\eta^5\text{-}C_5H_5)(\eta^5\text{-}C_5H_4(p\text{-}NH_2C_6H_5))$	708.2				
hydrolyzed I—slow[d]	708.3	153.7	102.6	6.26, 5.15	0.87, 0.99
hydrolyzed I—fast[d]	708.0	153.6	102.6	1.85, 3.64	1.18, 0.97
$Fe(\eta^5\text{-}C_5H_5)_2$	707.5				

[a] Relative to C 1s as 285.0 eV. [b] Ratio of band areas. [c] Repeated scanning of this sample showed no reductive beam damage. A diffuse satellite ~714 eV was observed for this sample. [d] I hydrolyzed by exposure of an isooctane solution of I to atmospheric moisture (slow), curve 5, Figure 3, or by deliberate injection of H_2O into isooctane solution of I (fast), curve 6, Figure 3; see Experimental Section.

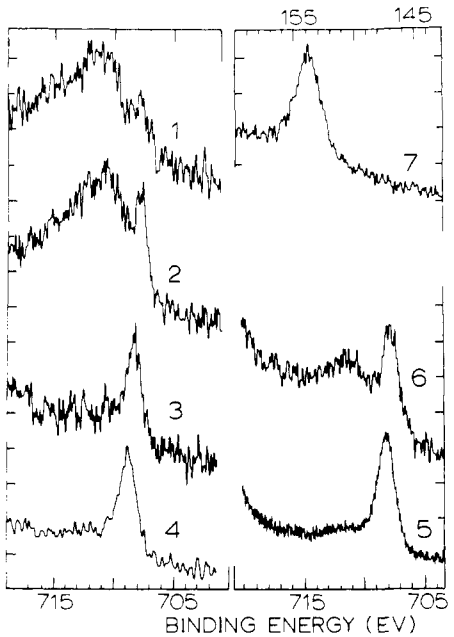

Figure 3. Fe $2p_{3/2}$ (curves 1-6) and Si 2s (curve 7) XPES bands on electrodes reacted with I and on polymerized I: Curve 1, electrode C of Table I (256 counts/div); curves 2, 7, electrode F (512 counts/div); curve 3, electrode B (512 counts/div); curve 4, 1,1'-ferrocenedicarboxylic acid (512 counts/div); curves 5, 6, polymerized I of Table II.

distinct in one of the polymerized samples of I (curve 6).

An extensive literature[7] exists on energy loss satellites for transition metals including those of Fe $2p_{3/2}$ spectra. Energy loss satellites of Fe $2p_{3/2}$ vary in intensity and spacing from the main peak, according to the ligand in Fe complexes. The satellite is typically separated from the main peak by 4-5 eV. Fe $2p_{3/2}$ energy loss effects normally, however, lead to satellites of considerably lower intensity than many of our spectral observations (e.g., curves 1, 2, and 6 of Figure 3). While the observed satellites might reveal uncommonly efficient energy loss processes, and vary as a result of the structural variations within the multilayers as suggested by the electrochemistry, we think that a chemical state interpretation of the satellites is more plausible.

XPES of a model ferricenium sample (Table II) shows a moderately broad $2p_{3/2}$ band at 710.6 eV. On the other hand, a mixed valence Fe(II), Fe(III) biferrocene spectrum[8] exhibits a sharp 707.7-eV band (Fe(II)) plus an equal intensity but quite diffuse 711.1-eV band (Fe(III)). The latter has the same appearance as the 711-eV band in Figure 6. Additionally, ferrocene derivatives attached to carbon surfaces by three other completely different chemistries[9a,b] also exhibit a broad 711-eV band, as well as the usual 708-eV ferrocene peak. In one case, we have shown that preliminary reductive treatment substantially eliminates the 711-eV band. Finally, binding I to a high surface area, transparent substrate[9c] reveals a blue-green (ferricenium) coloration of many specimens. These evidences lead us to interpret the broad 711-eV Fe $2p_{3/2}$ as a ferricenium state; e.g., the electrode preparation leaves a substantial fraction of the ferrocene sites in an oxidized state.

An alternate interpretation invoking differential charging of different ferrocene multilayer regions in the XPES experiment can be ruled out since the Si 2s and O 1s spectra exhibit no analogous satellites.

The efficiency of photoelectron production from ferrocene and ferricenium sites on electrodes coated with I should be the same. We have accordingly integrated the entire area of satellite plus main peak in the electrode bands as illustrated in Figure 3. This Fe $2p_{3/2}$ intensity is given relative to the substrate electrode metal (Pt or Au) in Table I. The ratio of intensities of iron and substrate electrode varies systematically with electrochemically measured coverage, an important result to which we will return.

The O 1s XPES on the ferrocene-multilayer electrodes was a single, somewhat broad, band whose intensity relative to that of electrode substrate is given in Table I. The binding energy of this band, 532.4 eV, is entirely consistent with silicon-bound oxygen[10] in accord with expectations of the mode of binding and polymerization of I on the electrodes.

XPES of oxidized but otherwise untreated Pt electrodes exhibits, Figure 4 (curve 4), a 4f doublet asymmetrically tailing on the high binding energy side as typical of Pt with a thin oxide layer.[11] In comparison, the "oxide" character of the Pt spectrum exhibited by the ferrocene multilayer electrode, Figure 4, curve 6, partially disappears upon reaction of the Pt surface with I. A similar and more dramatic effect is observed for the Au electrodes. Figure 4, curve 1, shows the Au 4f spectrum of the oxidized Au electrode; the spectrum is similar to that previously observed[12] on a similarly oxidized Au electrode. The measured 86.2 eV Au $4f_{7/2}$ binding energy agrees with that (85.9 eV) observed earlier and attributed to a layer of Au_2O_3 phase oxide. The oxide thickness is very approximately 15 Å. Interestingly, upon reaction of the oxidized Au electrode with I, these prominent oxide phase bands disappear, leaving a Au 4f spectrum (curve 3) of very nearly the same shape as that of an otherwise untreated Au electrode (curve 2). The oxide is clearly removed in the silanization reaction medium. Apparently, the population of surface Au and Pt atoms involved in -M-O-Si- bonding is insufficiently large to be perceptible in the spectrum.

All electrodes exhibit a single, broad Si 2s band whose appearance was similar from electrode to electrode (Figure 3). Intensities relative to Fe $2p_{3/2}$ given in Table I are also similar from electrode to electrode. Conversion of intensities to a stoichiometric Fe/Si atom ratio for the attached ferrocene layer involves relative XPES elemental sensitivities as established either experimentally with standard compounds or with theory. The latter involves the ratio $\sigma_{Fe}\lambda_{Fe,sil}/\sigma_{Si}\lambda_{Si,sil}$, where

σ is the photoelectron cross section[13] and λ is the escape depth for the respective element's photoelectrons in the ferrocene–silane layer. Using a model by Penn[14] which indicates that escape depths of photoelectrons depend on kinetic energy approximately as $\lambda \propto (KE)^{0.75}$, the theoretical relative sensitivity [Fe $2p_{3/2}$]/[Si 2s] is calculated at 7.26. An experimental relative sensitivity [Fe $2p_{3/2}$]/[Si 2s] = 9.06 calculated from the standard compound in Table II agrees reasonably well with the theoretical value.

Application of the 9.06 relative sensitivity ratio to the ferrocene electrode results yields an average atom stoichiometry of 0.26 Fe/Si. Although this result is approximate, its deviation from the ideal 1/1 ratio is sufficiently great to strongly suggest that the electrode surfaces are Fe poor. Perhaps oligomerization leads to expulsion of some ferrocene moieties, or oligomerization becomes terminated (i.e., ultimate coverage for a particular experiment achieved) by formation of a Si-rich siloxane layer at the ferrocene–solution interface. It is possible that this characteristic of the ferrocene multilayer plays an important role in the electrochemical properties.

XPES of hydrolyzed samples of I qualitatively accord well with the XPES of electrode surfaces derivatized with I in that the I_{Fe}/I_{Si} ratios reflect lower than 1/1 Fe/Si ratios in the sample, Table II. The variation in the I_{Fe}/I_{Si} ratios for the hydrolysis products suggests some inhomogeneity in the samples. Elemental analyses of hydrolysis products show Fe/Si ratios in the range of 0.33–0.36 for three different samples but the C/Fe and C/Si ratios show substantial variation reflecting complex hydrolysis processes. The main point is that deliberate reaction of I with H_2O or with the electrode surface results in Fe-deficient material and the electroactive materials attached to such surfaces cannot be strictly viewed as simple oligomers of ferrocenes linked by -Si-O-Si- bonds.

One of the most interesting aspects of the data of Table I is the correlation between the electrochemically measured coverage and the ratio of XPES intensities Fe/Pt and Fe/Au. For the purposes of the following discussion, Pt and Au are identified as a common electrode substrate element M; this is a reasonable assumption inasmuch as the kinetic energy of 4f photoelectrons from these two materials is nearly identical. If the bonded ferrocene multilayer is considered a homogeneous, smooth layer overcoat of thickness d, the intensity of electrode substrate M relative to that of an uncoated electrode of element M is given by

$$\frac{I_M}{I_M^0} = \exp[-d/\lambda_{M,sil}] \qquad (1)$$

where $\lambda_{M,sil}$ is the escape depth of the photoelectrons of M through the ferrocene/silane overlayer. Another relationship which can be derived for this layer model involves the relative intensities of ferrocene iron and M:

$$\frac{I_{Fe}\sigma_M n_M \lambda_{M,M}}{I_M \sigma_{Fe} n_{Fe} \lambda_{Fe,sil}} = \exp[d/\lambda_{M,sil}] - \exp[d/\lambda_{M,sil} - d/\lambda_{Fe,sil}] \qquad (2)$$

where n is atoms/cm^3 and λ is escape depth for the indicated element through the indicated medium. The thickness of the ferrocene overlayer, d, is related to the molar (mol/cm^2) coverage by ferrocene through the average molecular weight of the immobilized ferrocene derivative and its density:

$$d = 10^8(MW)\Gamma/D_{sil} \qquad (3)$$

where Γ is molar coverage and D_{sil} is the density of the ferrocene silane layer. We will for the present identify the actual molar coverage of iron with the electrochemically measured molar coverage.

Previous papers[11a,12,15] have correlated electrochemical coverages with XPES intensity ratios, but the situation represented by eq 2 is more complex than these early cases, since the overlayer and the substrate elements are different. This leads to escape depth and relative cross-section terms in eq 2 absent from the earlier situations.

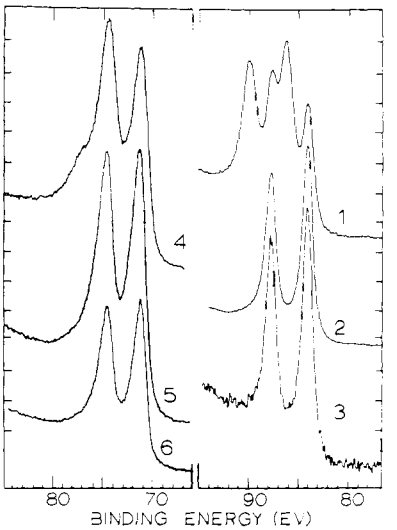

Figure 4. Au 4f XPES bands: curve 1, Au with Au_2O_3 overlayer (2048 counts/div); curve 2; untreated Au (4096 counts/div); curve 3, Au electrode F of Table I (256 counts/div). Pt 4f XPES bands: curve 4, oxidized Pt (1024 counts/div); curve 5, untreated Pt (2048 counts/div); curve 6, Pt electrode C of Table I (2048 counts/div).

Equation 2 was compared to the Fe/Pt and Fe/Au intensity data of Table I in the following manner. As an initial approximation, the extreme right-hand term of eq 2 was set equal to zero, and a plot made of ln $[I_{Fe}/I_M]$ vs. Γ; the resulting plot was reasonably linear. The intercept, $-\ln[\sigma_M n_M \lambda_{M,M}/\sigma_{Fe} n_{Fe} \lambda_{Fe,sil}]$, was dissected using theoretical cross sections for σ_M and σ_{Fe},[12] 14.3 Å for $\lambda_{M,M}$,[13] average $n_M = 6.3 \times 10^{22}$ atoms/cm^3 for Pt and Au, and a calculated[14] $\lambda_{Fe,sil} = 13.9$ Å, from which $n_{Fe} = 3.45 \times 10^{21}$ atoms/cm^3. From this result, taking MW = 244 ($C_{10}H_8SiO_2Fe$), a density of the ferrocene silane layer $D_{sil} = 1.40$ g/cm^3 is calculated. Considering that the density of ferrocene itself is 1.49 g/cm^3, and that measured for hydrolyzed I is 1.61 g/cm^3, this result is reasonable. The derived density is next employed with the plot's slope to estimate $\lambda_{M,sil} = 37$ Å, from which the extreme right-hand term of eq 2 was next calculated as a correction factor (it proves to be nearly negligible, ranging from 0.28 at low Γ to nearly zero at high Γ) and eq 2 replotted. Figure 5 shows that the variation of relative XPES Fe/M intensities correlates quite well with electrochemically determined coverage. Ferrocene silane thicknesses calculated from XPES data with eq 2 and from electrochemical coverages using eq 3 and $D_{sil} = 1.4$ are listed in Table I.

Using the estimate of $\lambda_{M,sil} = 37$ Å, values of ferrocene–silane thickness d were also calculated from eq 1 and are listed in Table I. Considering that the latter calculation contains the uncertainty of comparing intensities measured on two separate electrode specimens, the correspondence between two different XPES analyses of d, by eq 1 and 2, is quite satisfactory. Furthermore, a theoretical calculation[14] of the escape depth $\lambda_{M,sil}$ yields 26 Å, which, considering the accumulation of approximations made, is in respectable agreement with the experimental value 37 Å.

Two interesting features emerge from this analysis of the experimental data. First, apparent dimensions of the attached ferrocene silane overlayer are quite large. According to the analysis of Table I, electrochemistry on the electrode with highest coverage corresponds to charge transfer through well over 100 Å of ferrocene–silane. It should be expected in such

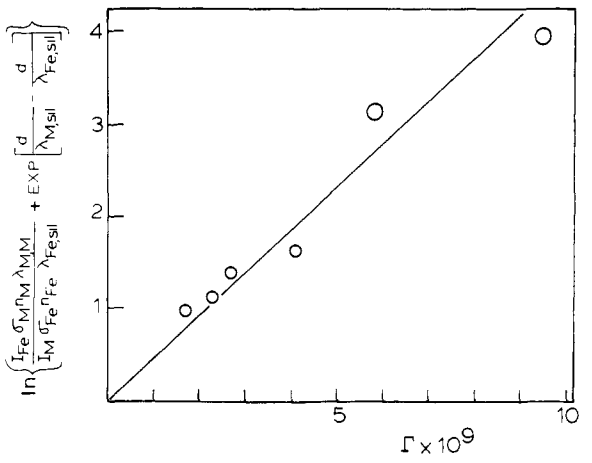

Figure 5. Plot of Fe $2p_{3/2}$ and $M_{5/2+7/2}$ relative XPES intensities in rearranged eq 2 vs. electrochemically measured coverage Γ, using parameters $\lambda_{M,M}$ = 14.3 Å, $\lambda_{Fe,sil}$ = 13.9 Å, $\lambda_{M,sil}$ = 37 Å, $n_M = 6.3 \times 10^{22}$ atom/cm³, and $n_{Fe} = 3.45 \times 10^{21}$ atoms/cm³.

a situation that the prerequisites for charge transfer are stringent and require both facile counterion mobility and a reasonably open structure. The dependence of the electrochemical behavior on the counterion in a comparison of perchlorate and tetraphenylborate[3] and the variability of electrochemical reversibility from preparation to preparation are consistent with this view.

Secondly, the correspondence of an electrochemically measured quantity of ferrocene with a XPES-measured quantity of iron, Figure 5, indicates that to at least a first approximation all of the iron present is ferrocene iron and that all of the ferrocene iron is electroactive in the electrochemical experiment. This assertion has, of course, limitations with respect to the accuracy of the data fit represented in Figure 5, plus the uncertainties associated with its assumption that the ferrocene–silane film has a uniform thickness. XPES relations which assume simple forms of nonuniformity (such as metal-exposing pores), when compared to eq 1 and 2, show I_M/I_M^0 and I_{Fe}/I_M to be decreasingly responsive to film thickness at larger pore areas and at larger thicknesses. Model calculations indicate that effects of pores of area 10% of the total (causing ca. 30% error in d) could be accommodated within the data scatter. More extreme porosity would appear to be ruled out.

Acknowledgment. Research at the University of North Carolina was supported by the National Science Foundation and the Office of Naval Research and at Massachusetts Institute of Technology by the U.S. Department of Energy, Office of Basic Energy Sciences. We also thank J. R. Lenhard for useful discussions and Professor W. F. Little for generous gifts of a variety of ferrocene derivatives.

References and Notes

(1) (a) Massachusetts Institute of Technology; (b) University of North Carolina.
(2) (a) J. R. Lenhard and R. W. Murray, *J. Electroanal. Chem.*, **78**, 195 (1977); (b) M. S. Wrighton, R. G. Austin, Andrew B. Bocarsly, J. M. Bolts, O. Haas, K. D. Legg, L. Nadjo, and M. C. Palazzotto, *ibid.*, **87**, 429 (1978).
(3) M. S. Wrighton, M. C. Palazzotto, A. B. Bocarsly, J. M. Bolts, A. B. Fischer, and L. Nadjo, *J. Am. Chem. Soc.*, **100**, 7264 (1978).
(4) R. F. Lane and A. T. Hubbard, *J. Phys. Chem.*, **77**, 1401 (1973).
(5) P. R. Moses, L. M. Wier, and R. W. Murray, *Anal. Chem.*, **47**, 1882 (1975).
(6) W. S. Woodward, J. L. Hinderliter-Smith, E. S. Brandt, and C. N. Reilley, in preparation.
(7) (a) S. Larsson, *Chem. Phys. Lett.*, **40**, 362 (1976); (b) T. A. Carlson, J. C. Carver, L. J. Keathre, F. G. Santibanez, and G. A. Vernon, *J. Electron Spectrosc. Relat. Phenom.*, **5**, 247 (1974); (c) B. Walbank, I. G. Main, and C. E. Johnson, *ibid.*, **5**, 259 (1974); (d) J. C. Carver, G. K. Schweitzer, and T. A. Carlson, *J. Chem. Phys.*, **57**, 973 (1972); (e) T. A. Carlson, J. C. Carver, and G. A. Vernon, *ibid.*, **62**, 932 (1975).
(8) D. O. Cowans, J. Park, M. Barber, and P. Swift, *Chem. Commun.*, 1444 (1971).
(9) (a) D. F. Smith, K. Willman, K. Kuo, and R. W. Murray, *J. Electroanal. Chem.*, **95**, 217 (1979); (b) R. Nowak, F. A. Schultz, M. Umana, H. Abruna, and R. W. Murray, *ibid.*, **94**, 219 (1978); (c) R. H. Staley, J. B. Kinney, A. B. Fischer, and M. S. Wrighton, submitted for publication.
(10) P. R. Moses, L. M. Wier, J. C. Lennox, H. O. Finklea, J. R. Lenhard, and R. W. Murray, *Anal. Chem.*, **50**, 576 (1978).
(11) (a) J. S. Hammond and N. Winograd, *J. Electroanal. Chem.*, **78**, 55 (1977); (b) K. S. Kim, N. Winograd, and R. E. Davis, *J. Am. Chem. Soc.*, **93**, 6296 (1971).
(12) T. Dickinson, A. F. Povey, and P. M. A. Sherwood, *J. Chem. Soc., Faraday Trans. 1*, **71**, 298 (1975).
(13) J. H. Scofield, *J. Electron Spectrosc. Relat. Phenom.*, **8**, 129 (1976).
(14) D. R. Penn, *J. Electron Spectrosc. Relat. Phenom.*, **9**, 29 (1976).
(15) T. A. Carlson and G. E. McGuire, *J. Electron Spectrosc. Relat. Phenom.*, **1**, 161 (1972–1973).

Spectra of the H_2 Phthalocyanine in Low-Temperature Matrices

V. E. Bondybey* and J. H. English

Contribution from Bell Laboratories, Murray Hill, New Jersey 07974.
Received July 17, 1978

Abstract: Laser emission and excitation spectra of H_2 phthalocyanine in solid Ar and Ne matrices were examined. The spectra display a sharp vibronic structure, both in excitation and emission. Polarization studies confirm the presence of two overlapping transitions in the red. It is suggested that a strong vibronic coupling is responsible for the appearance of several perpendicularly polarized bands below the Q_y origin.

I. Introduction

Porphyrin-type molecules are an extremely important class of compounds with a a key role in photosynthesis, oxygen transport, and other biologically important reactions. Their properties are therefore of great interest and over the years they were frequently studied by a variety of spectroscopic tools. Only in the last 5 years more than 200 publications dealt with the subject of phthalocyanine alone. The spectra of porphyrins were extensively studied in a variety of organic solvents. In particular, works by Gorokhovskii, Personov, and others in Spolskii matrices provided extensive information.[1-7]

The electronic spectroscopy of porphyrins is characterized

0002-7863/79/1501-3446$01.00/0